INL/JOU-24-79785-Revision-0

Modeling and Optimization of a Nuclear Integrated Energy System for the Remote Microgrid on El Hierro

November 2024

Logan David Williams, Daniel Mark Mikkelson, J. Michael Doster

Changing the World's Energy Future

Idaho National Laboratory

INL is a U.S. Department of Energy National Laboratory operated by Battelle Energy Alliance, LLC

INL/JOU-24-79785-Revision-0

Modeling and Optimization of a Nuclear Integrated Energy System for the Remote Microgrid on El Hierro

Logan David Williams, Daniel Mark Mikkelson, J. Michael Doster

November 2024

Idaho National Laboratory
Idaho Falls, Idaho 83415

http://www.inl.gov

Prepared for the
U.S. Department of Energy
Under DOE Idaho Operations Office
Contract DE-AC07-05ID14517

energies

MDPI

Article

Modeling and Optimization of a Nuclear Integrated Energy System for the Remote Microgrid on El Hierro

Logan Williams [1,2,*], J. Michael Doster [2] and Daniel Mikkelson [1]

[1] Idaho National Laboratory, Idaho Falls, ID 83415, USA; daniel.mikkelson@inl.gov
[2] Department of Nuclear Engineering, North Carolina State University, Raleigh, NC 27695, USA; doster@ncsu.edu
* Correspondence: logan.williams@inl.gov

Abstract: Nuclear microreactors are a potential technology to provide heat and electricity for remote microgrids. There is potential for the microgrid on the island of El Hierro to use a microreactor, within an integrated energy system (IES), to generate electricity and provide desalinated water. This work proposes a workflow for optimizing and analyzing IESs for microgrids. In this study, an IES incorporating a microreactor, thermal energy storage (TES) system, combined heat and power plant, and a thermal desalination plant was designed, optimized, and analyzed using Idaho National Laboratory's Framework for Optimization of Resources and Economics (FORCE) toolset. The optimization tool, Holistic Energy Resource Optimization Network (HERON), was used to determine the optimal capacity sizes and dispatch for the reactor and thermal energy storage systems to meet demand. The optimized reactor and TES sizes were found to be 11.61 MW_{th} and 58.47 MWh_{th}, respectively, when optimizing the IES to replace 95% of the island's existing diesel generation needs. A dynamic model of the system was created in the Modelica language, using models from the HYBRID repository, to analyze and verify the dispatch from the optimizer. The dynamic model was able to meet the ramp rates while maintaining reactor power with minimal control adjustments.

Keywords: microgrid; microreactor; Modelica; integrated energy systems; thermal energy storage; desalination

Citation: Williams, L.; Doster, J.M.; Mikkelson, D. Modeling and Optimization of a Nuclear Integrated Energy System for the Remote Microgrid on El Hierro. *Energies* **2024**, *17*, 5826. https://doi.org/10.3390/en17235826

Academic Editors: Dan Gabriel Cacuci and Gediminas Stankūnas

Received: 14 September 2024
Revised: 31 October 2024
Accepted: 19 November 2024
Published: 21 November 2024

1. Introduction

Microgrids are a network of distributed energy resources (DER) and loads within clearly defined electrical boundaries that act as a single controllable entity [1]. There are two main types of microgrids: connected and remote. Connected microgrids are typically connected to a major electrical grid but can also operate in island mode where the generation and storage in the system provide all the microgrid's power requirements. Remote microgrids are physically disconnected from any large grid and always operate in island mode. Remote microgrids can provide heat and power for communities, mining operations, industrial facilities, and military bases in remote locations. These remote communities exist where it is difficult or not economically viable to connect to a larger grid, such as on small islands or in rural areas such as Alaska, which alone has more than 110 remote microgrids [2]. Microgrids can also provide power to regions of the world that do not have a large-scale energy grid, such as sub-Saharan Africa. Currently, diesel is the main source of power for these microgrids, with increasing use of renewables where possible. In the case of remote microgrids, fuel costs are significantly higher, making electrical costs higher [2]. One proposed solution for reducing costs, as well as increasing grid resilience, is the use of microreactors. These small nuclear reactors could be capable of providing cheaper clean energy to these communities [3,4].

Due to the nature of microgrids, a nuclear reactor will likely operate differently than it typically does on a large grid. The small number of users and limited availability of DERs causes larger relative fluctuations in demand, which can be further compounded by the

variation in supply from intermittent energy sources, such as wind and solar. Integrated energy systems (IES) are cooperatively controlled energy systems that are able to better utilize heat and power from one or multiple energy systems [5]. An IES can both help utilize the power from a microreactor more efficiently in these environments as well as make additional use of the heat source provided by the reactor itself for other applications, such as desalination, home heating, or chemical production. Due to the large capital cost of these systems, it will be important to size them correctly to minimize the overall cost of energy while still having a system that can reliably meet demand.

Many tools exist to aid in the design and optimization of microgrids [6], including HOMER (Hybrid Optimization Model for Electric Renewables) [3], PLEXIOS Microgrid [7], Xendee [8], SER-CAM (Distributed Energy Resources Customer Adoption Model) [9], and OSeMOSYS (Open-Source Energy Modeling System) [10]. Most work with these tools, or similar methods, do not consider nuclear as an option, though a few studies have extended them to look at microreactors for microgrids [11–14]. Even fewer studies have looked at optimizing nuclear remote microgrid IESs [3].

As part of United State Department of Energy's IES program, the Framework for Optimization of Resources and Economics (FORCE) has been developed to help design, optimize, and analyze IESs [15,16]. This work expands the use of these tools for remote microgrids with a workflow for optimizing and analyzing IESs for microgrids with FORCE tools. A more detailed description of FORCE is provided in Section 2.1. The novel contributions from this work are listed below:

- Presents a real microgrid scenario.
  - A microreactor-powered IES microgrid was designed to provide electricity and process heat for desalination to help meet the power and water demands of the island.
- Novel use of FORCE tools for remote microgrid applications.
  - This method uses stochastic time series data to help account for uncertainty for future demand and generation.
  - The optimization results are analyzed, quantifying the uncertainty in this optimization method.
- A dynamic physical model of the microgrid was created.
  - A dynamic model of the nuclear IES microgrid was created.
  - The simplistic surrogate models used by the optimizer are compared to dynamic physics-based models.
  - Reactor stability is analyzed with a dynamic multiphysics model.

1.1. Microreactors

Microreactors are normally considered to be below 20 MW_e [4]. Their small size expands the application range of nuclear energy to regions where gigawatt-scale plants are inappropriate. One attractive quality of microreactors over other low-carbon energy sources is that they offer access to a large heat source. IESs can take advantage of this heat source by using it for auxiliary applications along with electric power generation.

High-temperature gas-cooled reactors (HTGRs) use gas as the primary coolant and operate at higher temperatures (750–950 °C) than light-water reactors. Designs for both thermal and fast gas-cooled reactors are actively being developed [17]. The thermal spectrum designs are further along with several have already been built globally. HTGRs can also be further categorized by fuel geometry, either prismatic block or pebble bed. The prismatic HTGR is a common design type for microreactors due to its high technology-readiness level, making it an attractive choice for a near-term deployment scenario. For this work, a prismatic HTGR was chosen as the reactor.

1.2. El Hierro, Canary Islands, Spain

The Canary Islands are an autonomous community of Spain, 100 km off the west coast of Morocco. There are seven main islands with a combined population of more than 2.1 million people. Access to freshwater resources varies from island to island, with some islands being water scarce [18]. Several of these islands currently use desalination to help meet freshwater demand. It is likely that this capacity will need to be expanded in the future as the demand for fresh water increases in the islands [18].

El Hierro (Figure 1) is the smallest of the seven main Canary Islands, both in area (258.5 km^2) and population (11,338). Currently, its residents' freshwater needs are met with groundwater and three desalination plants. The need for desalinated water is expected to continue to grow [18]. The electrical grid on El Hierro is an isolated microgrid that is not connected to the grids of any of the other islands or the mainland. Currently the island relies on a mix of wind and diesel power, with an average electrical demand of 5.6 MW_e [19]. The electricity demand and wind generation profile for a year is shown in Figure 2. There is also a pumped hydro storage (PHS) system on the island.

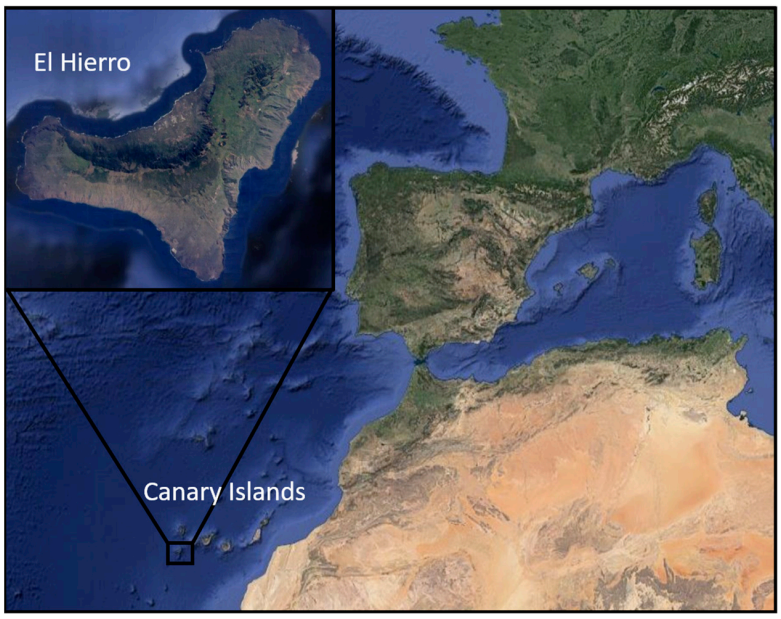

Figure 1. Location of El Hierro, Canary Islands, Spain. Maps Data: Google 2024 [20].

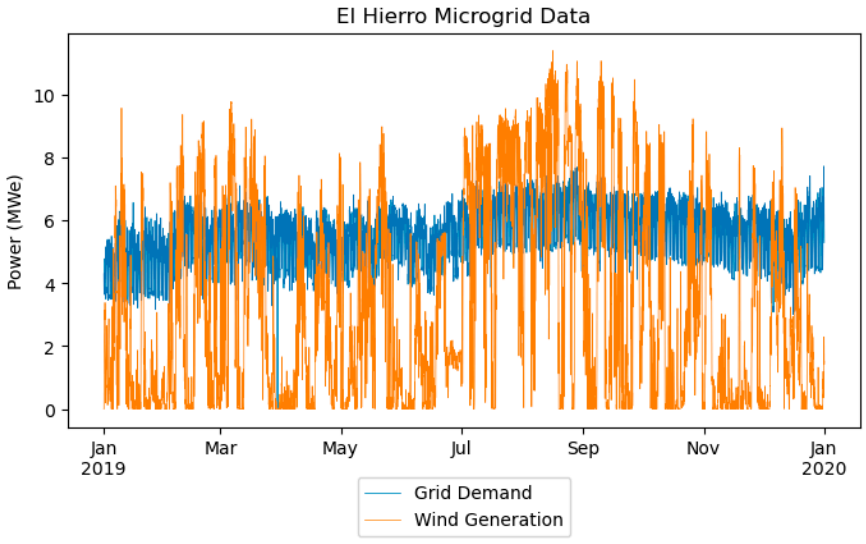

Figure 2. El Hierro electricity demand and wind generation for a year [19].

This deployment scenario examines replacing diesel generation on the island with a microreactor. The reactor is connected to a thermal energy storage (TES) system, which dispatches heat to a combined heat and power (CHP) plant to produce electricity and heat, as illustrated in Figure 3. The heat will be used to power a thermal desalination plant using a multi-effect evaporator (MEE) system. While reverse osmosis (RO) desalination systems are typically more efficient than thermal systems such as MEEs, they require comprehensive pretreatments for use with high-saline water, such as seawater, and produce less pure water with a higher output salinity [21]. MEEs also require less maintenance, are simpler to operate, and can directly use low-grade heat. For these reasons, MEE systems may be a better option for remote microgrids where the limited infrastructure and resources may make the operation of RO systems much more complex. Due to these considerations, an MEE system was chosen as the desalination technology in this deployment scenario. The MEE system will operate at a constant water production rate and will nominally use low-temperature steam (120 °C).

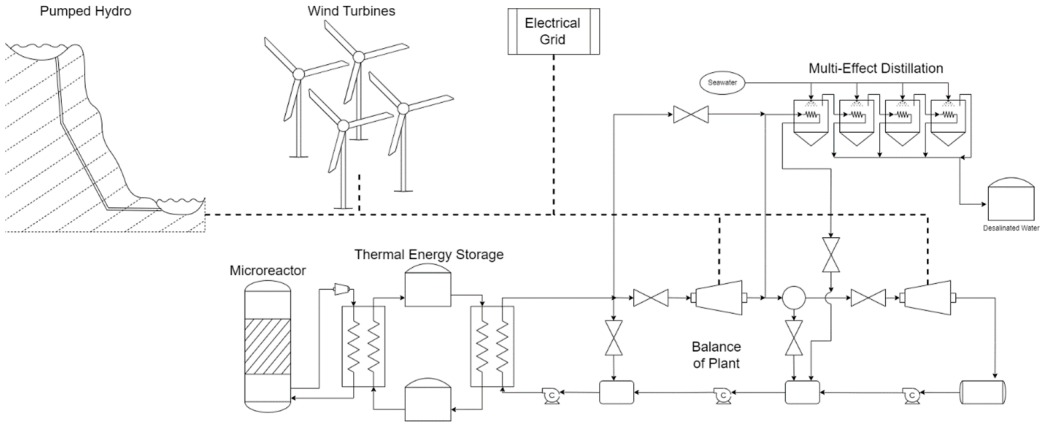

Figure 3. Block diagram of El Hierro IES.

The island's installed wind capacity is sufficient to cover its entire electricity demand on windy days, but the wind capacity is not enough on calm days, leading to heavy reliance on dispatchable diesel power. The pumped hydro on the island can store excess power on windy days and supplement generation on days with no wind. This scenario presents an interesting optimization case for replacing diesel with nuclear, while increasing freshwater access.

The "nuclear island" consists of an HTGR microreactor, a two-tank TES system, an intermediate heat exchanger (IHX), and a steam generator. Heat from the microreactor is transported through the primary helium coolant to the IHX. Heat is transferred across the IHX to molten salt, which is stored in the hot tank. The molten salt is dispatched from the hot tank through a steam generator, producing steam and returning to the cold tank based on system demand. A once-through steam generator was chosen to create superheated high-pressure steam for the CHP plant. The system is designed to operate the reactor at a constant power, constantly charging the TES system, while the TES system discharges to follow the combined electric and thermal load. Figure 4 is a block diagram of the nuclear island.

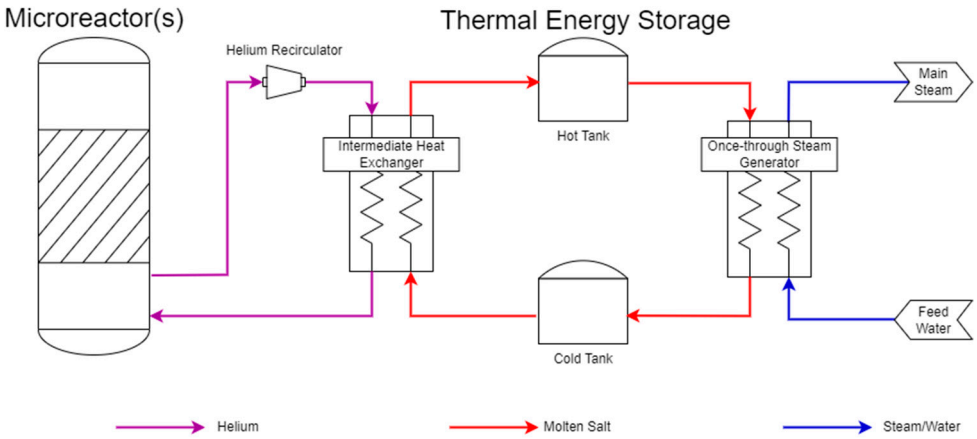

Figure 4. Nuclear island block diagram.

2. Materials and Methods

This section introduces the tools used in this work, as well as the workflow developed.

2.1. Framework for Optimization of Resources and Economics

Idaho National Laboratory (INL) has conducted research into nuclear power IES as part of the U.S. Department of Energy's Integrated Energy Systems Program. This work has included both computational and experimental research into many of the technical aspects of IES, such as TES, high-temperature steam electrolysis, and thermal integration [22–25]. A significant amount of research has looked at the economics of these systems [24,26,27]. To support this effort, the Framework for Optimization of Resources and Economics (FORCE) toolset has been developed, consisting of Risk Analysis Virtual Environment (RAVEN), Holistic Energy Resource Optimization Network (HERON), Feasible Actuator Range Modifier (FARM), Tool for Economic Analysis (TEAL), and the HYBRID model repository [15,16]. This work used HYBRID, RAVEN, and HERON, each of which are described in the following sections.

2.1.1. HYBRID

HYBRID is an open-source repository of system models, primarily transient physical models written in the Modelica language, using the commercial Dymola compiler. Modelica is an acausal, inherently dynamic, and object-oriented development language. Energy system models including nuclear reactors, industrial processes, balance of plants (BOPs), and more are in this repository, allowing for large IESs to be modeled and studied [28,29].

2.1.2. Risk Analysis Virtual Environment

RAVEN is a multipurpose uncertainty quantification, regression analysis, probabilistic risk assessment, data analysis, and model optimization framework. It can sample and execute a wide variety of software packages and then use the data gathered for different operations, such as creating reduced order models (ROMs) or statistical analysis [30,31]. RAVEN was used in this work to create ROMs and sample Dymola models.

2.1.3. Holistic Energy Resource Optimization Network

HERON is a modeling toolset for the optimization and technoeconomic assessment of various energy systems [32,33]. HERON can use surrogate models to create a network of resources that it can optimize. These surrogate models are sets of relationships between resource types. These models can also include limits, such as generation capacity, storage capacity, ramp rates, and minimum generation. The optimization process incorporates an inner and outer loop. The outer loop optimizes the IES by perturbing values in the surrogate model, such as generation capacity or storage capacity. With information from an outer loop iteration, the inner loop uses the model and demand data to generate a dispatch

profile for a given time horizon, typically several years with hourly intervals. With the dispatch profile, the inner loop can calculate the economic output of the system. This value is used as the target variable for the outer optimization loop, which typically tries to maximize the net present value (NPV) of the system, using a Bayesian optimizer.

The inner optimization is performed for a given project time and is broken down into clusters. In this case, the project time was set to be 4 years, and the cluster was set to be 120 h (5 days). For each cluster, the dispatch is solved independently in parallel.

The core of the HERON input file consists of components. Each component is a surrogate model representing a part of an IES. A component can produce, consume, transfer, or store one or more resources. The capacities of each of these components can be a fixed value, a swept value, or an optimized value. Each component can be either fixed or independent. A fixed dispatch sets the output to be a constant value at all times. Independent dispatch allows for the output to be varied by the inner optimizer to optimize the dispatch. For storage components, there is an additional parameter for periodic or nonperiodic storage. Periodic storage makes it so that the final storage level is equal to the initial storage level. Periodic storage is needed because the dispatch for each cluster is solved independently without any knowledge of the previous or next cluster. Economic values, such as capital costs (CAPEX), component lifetime, variable operations and maintenance costs (OPEX), and fixed operating and maintenance costs, can also be imputed for each component. These are used to calculate the desired resulting economic values such as NPV that will be used by the optimizer.

Figure 5 shows the HERON workflow. With the autoregressive-moving-average (ARMA) ROMs for demand/generation and surrogate models, a HERON input file is created. HERON will use this input file to generate a RAVEN input file of the outer optimization loop. This outer loop optimizes the component variables, such as capacity to maximize the NPV of the system. To find the NPV of the system with a given set of component sizes, the outer loop creates and automatically runs another RAVEN input file for an inner loop. This inner loop uses the ARMA ROM to create a set of histories. Then, each synthetic history is broken into years and clusters, with each year having one or more clusters. For each cluster, the optimized dispatch for each component is found. From this, the total NPV for each set of histories can be determined. The mean NPV of the set of histories is used to inform the outer loop optimizer. With this mean, value the outer loop perturbs the component variables and generates a new inner loop with a new set of synthetic histories [34].

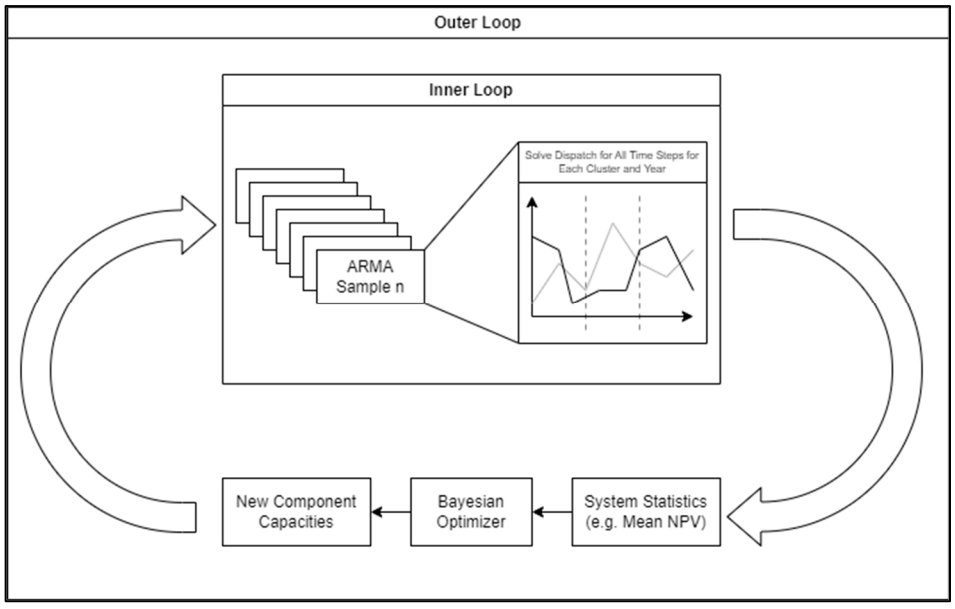

Figure 5. HERON workflow block diagram.

2.2. Workflow

Figure 6 depicts the proposed workflow for researching IESs for different microgrids. Using existing and newly created models from HYBRID, a dynamic systems model for each scenario will be created. From this model, a system network and surrogate models will be created for the HERON input file. Historical data from El Hierro was used to train a ROM using ARMA models. With the surrogate models; ARMA ROMs; and additional economic data, such as capital costs and operational costs, the full HERON input file will be created. With this, the microgrid will be optimized using the Bayesian optimizer built into RAVEN and HERON. HERON will also create the dispatch profiles for each component, such as the wind turbines, TES, microreactor, and BOP. Using the demand profiles for the ARMA ROMs as inputs for the dynamic models, the results of the HERON dispatch can be analyzed and validated against the full dynamic model.

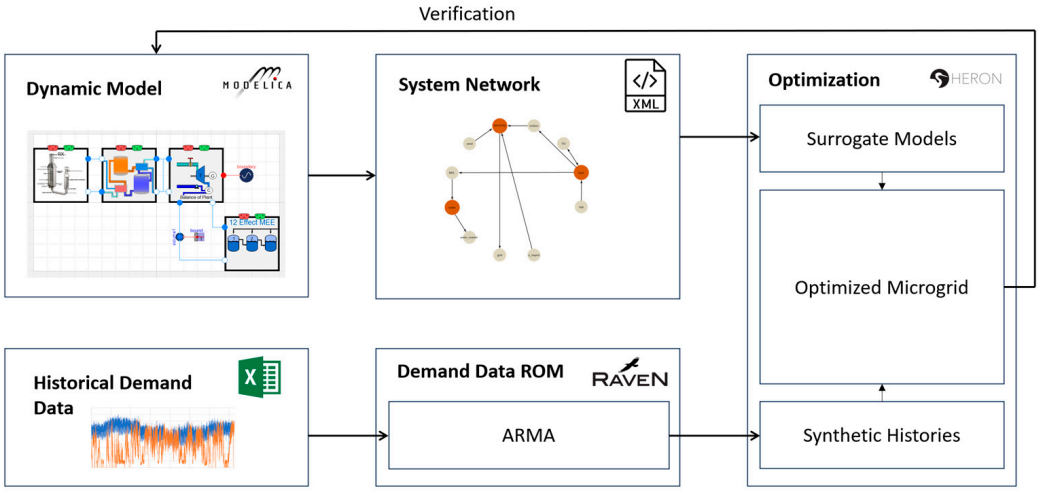

Figure 6. Workflow diagram.

2.3. Modeling

Models from the HYBRID repository were used to create a dynamic model of the microgrid IES. Models that used this work were developed in the Modelica language and are able to simulate the transient behavior of the IES.

2.3.1. Prismatic HTGR Microreactor

A prismatic HTGR reactor model from HYBRID was used for the microgrid IES dynamic model. This reactor model simulates the primary loop of the reactor while taking into account the feedback mechanisms of the core [35]. This model provides the heat source, for which energy will be transferred through the TES system to be converted to electricity and clean water via the BOP and MEE system.

2.3.2. Multiple Effect Evaporator

An MEE model was used to model the thermal desalination plant. This model uses a cascade of dual two-phase heat exchangers connected to boiling volumes to purify saltwater [36].

2.3.3. Balance of Plant

A modified version of an existing BOP model in HYBRID was used as the CHP plant to generate electricity and dispatch heat from an extraction point to the MEE system. During nominal operation, steam is extracted from between the high- and low-pressure sections of the turbine and sent to the MEE system. If the electrical demand of the microreactor is sufficiently low, to the point where the demand steam flow rate through the turbine is

exceeded by the MEE system's demand, the main steam is diverted instead of using an extraction line.

2.3.4. Thermal Energy Storage

A TES model from the HYBRID repository was used [37]. It is modeled as two fluid volumes, one for the hot tank and the other for the cold tank. Solar salt is used as the storage media, and it exchanges heat through a charging and discharging heat exchanger.

2.3.5. Control Systems

The complete control system can be seen in Figure 7. Control rods and a helium circulator control reactor power. The control rods maintain the core exit temperature, and the helium circulator controls the power level of the reactor. The two-tank molten salt TES has two control valves: the charging heat exchanger valve (CHXV) controls the flow through the charging heat exchanger, which is interfacing with the reactor, and the discharging heat exchanger valve (DHXV) controls flow through the discharging heat exchanger, which is connected to the BOP. The CHXV is used to maintain the hot tank inlet temperature. The DHXV is used to maintain the pressure in the steam generator (discharging heat exchanger). The BOP has several valves and pumps to control the system and allow it to meet both electrical and heat demand. The turbine control valve (TCV) is used to control the turbine output power to meet demand. The feed heating valve (FHV) is used to maintain feed water temperature by bypassing main steam to the second open feedwater heater. While feedwater temperature is typically not controlled in nuclear power plants, a control system was added in these models to ensure that the feedwater conditions going to the steam generator remain within their design limits in order to guarantee minimum salt temperature is maintained, as well as to prevent thermal cycling [38]. The third feedwater pump (FWP3) controls the flow rate through the cycles and is used to maintain the exit temperature of the steam generator. An extraction control valve (ECV) was placed between the sections of the turbine because the pressure at the inlet of the turbines is heavily dependent on the flow rate through the system, and this flow rate changes significantly with extraction for heat applications. The intermediate bypass valve (IBV) is used to control the heat application. For the MEE system, the IBV is used to maintain clean water production. All control variables and actuators are shown in Table 1. This control system is consistent with other dynamic modeling efforts using HYBRID.

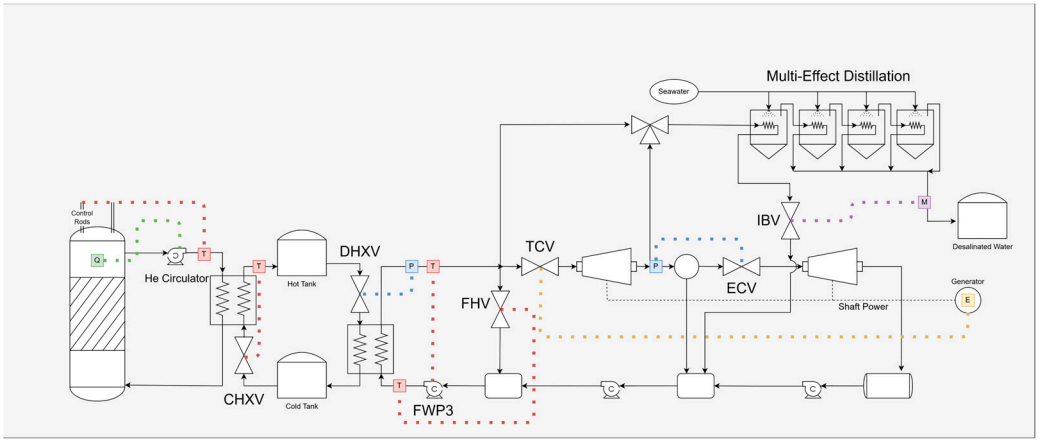

Figure 7. Control system diagram.

Table 1. Control system variables and set points.

Actuator	Controlled Variable	Nominal Set Point
Control Rods	Core Coolant Exit Temperature	630 °C
He Circulator	Reactor Power	Match Demand
Charging HX Valve	Hot Tank Inlet Temperature	565 °C
Discharging HX Valve	Steam Generator Pressure	120 bar
Turbine Control Valve	Electrical Power	Match Demand
Feed Heating Valve	Feed Water Temperature	200 °C
Feed Water Pump	Steam Temperature	540 °C
Extraction Control Valve	Extraction Pressure	3 bar
Intermediate Bypass Valve	MEE Water Production	8 kg/s

2.4. Microgrid Model

A complete microgrid was modeled with the microreactor, TES, BOP, and heat application. The Modelica model for microgrid is shown in Figure 8. Historical electrical demand data were used as the input demand for the model, and a constant demand of 8 kg/s, or ~10% of current freshwater usage, was used for the MEE system. This amount was chosen as it is low enough to not overly reduce the efficiencies of the CHP plant while still being enough to provide a significant amount of fresh water. Realistically, any amount of water production could be chosen, though it would affect the overall efficiency of the system. Increasing the amount of water production would cause the BOP to operate in bypass mode rather than extraction mode more often or would require the BOP to be redesigned as a back-pressure configuration.

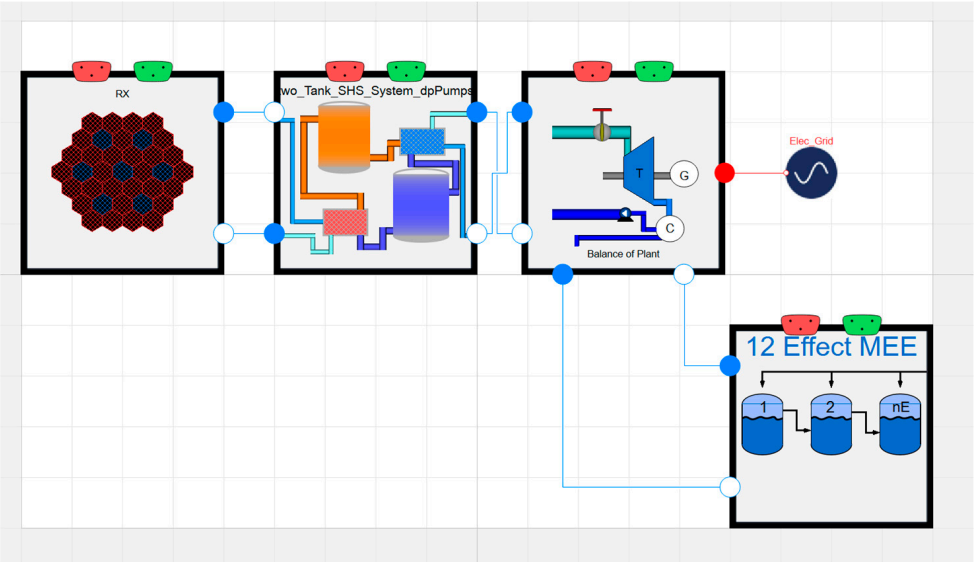

Figure 8. El Hierro microgrid Modelica model.

Additional Controls

In addition to the nominal control system, there are other system controls to prevent the TES from overfilling or emptying completely. For the overfilling case, there are two options: reduce reactor power or bypass steam to the condenser. Bypassing steam is the simplest but wastes some of the reactor fuel. The condenser system must also be sized adequately for this purpose. The other option of reducing reactor power can also present challenges. While load following is possible, there are physical constraints to ramp rates and ramp frequencies due to fission product poisons, such as Xe-135. Additionally,

frequent power adjustments will increase the wear on certain system components and increase reliance on operators, which in a remote microgrid scenario may be located far from the microreactor.

2.5. Optimization

2.5.1. Data Generation

To avoid the "golden year" problem, in which an optimizer can optimize for a single rare event rather than more common trends, a large number of datasets is needed to optimize the IES. As we only had data for a limited number of years for El Hierro's microgrid, synthetic data were needed. Synthetic data were obtained by training a ROM on real data. For electrical demand and wind generation, this was performed using an ARMA model with Fourier signal processing in RAVEN. This method uses real, historic data to train a ROM, which can create statistically similar, but unique, demand profiles for arbitrary time periods.

A ROM for electrical power demand profiles and wind generation was trained with real power data from El Hierro [19]. Figure 9 is a heat map of a large number of electrical demand signals created by the ARMA ROM.

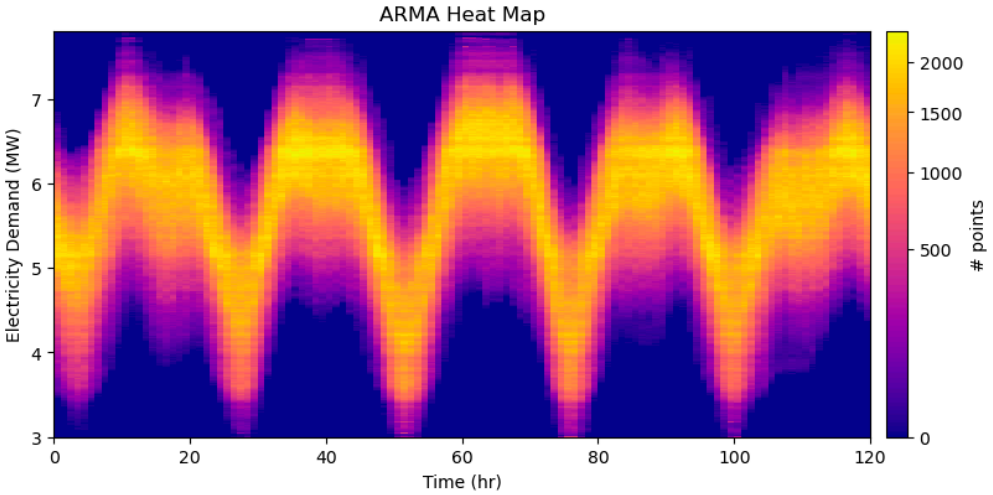

Figure 9. Heat map of synthetic data from El Hierro (n = 292,000 clusters).

2.5.2. HERON Input File

A HERON input file requires a set of information for each component in the system. This set of information creates a surrogate model for the optimizer to use. Because of the large number of calculations performed, these are very simple models. The inputs for the surrogate models are typically the resources a component produces or demands, capacity limits, and economic data. In this scenario, the microreactor and TES size are the components that were optimized. As HERON is an economic optimizer, costing information is needed for many of the components. Microreactor costs were taken from Abou-Jaoude et al. (2023) using the medium level cost estimates [39]. The TES costs were taken from Gautam, Andresen, and Victoria (2022) [40], and only the energy CAPEX and OPEX were used as it is assumed that the power CAPEX is part of the reactor CAPEX; the same is assumed for the BOP component. The MEE system does not have any cost associated with it as it is the same size all HERON runs that were performed for this study. Because this and other associated costs were not used in this analysis, the absolute NPV of the system is somewhat meaningless, but the change in NPV is not, so for this analysis, only Δ NPVs are reported. Table 2 tabulates the components in the HERON input file, and Figure 10 is a diagram of the system as modeled in HERON.

Table 2. HERON input file components.

Component	Component Type	Resource	Capacity
Reactor	Source	Heat	Opt
BOP	Transfer	Heat, Electricity	Fixed
MEE	Transfer	Heat, Water	Fixed
TES	Storage	Heat	Opt
Diesel	Source	Electricity	Fixed
Wind	Source	Electricity	ARMA
PHS	Storage	Electricity	Fixed
Grid	Sink	Electricity	ARMA
Water Market	Sink	Water	Fixed

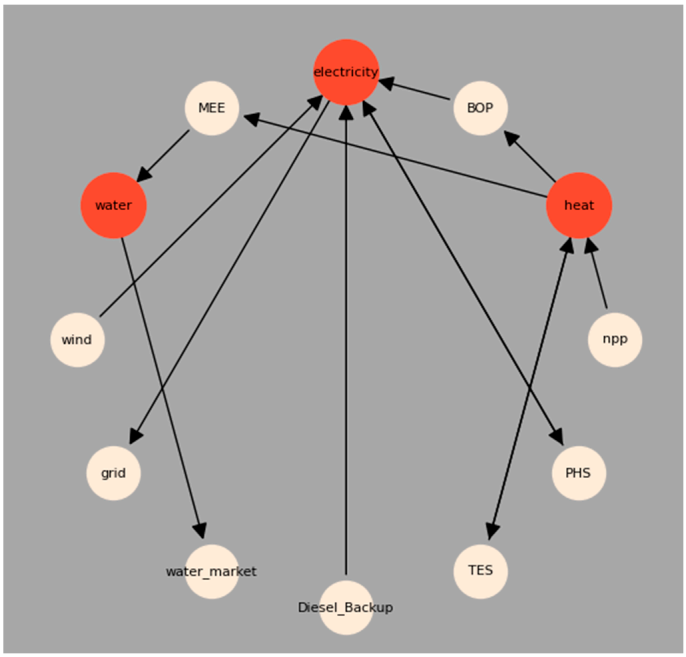

Figure 10. HERON input file network.

The HERON file is set up to run a 4-year analysis with 200 ARMA samples. TES systems have 30-year operating lifetimes, and advanced reactor systems are expected to have 60-year or longer lifetimes. As such, to obtain an accurate Δ NPV to compare between systems, lifetime costs were annualized within the actual HERON input.

The following equation was used to modify the capital costs.

$$C_{actual} * \frac{i \cdot (i+1)^{t_1}}{(i+1)^{t_1} - 1} = C_{modified} * \frac{i \cdot (i+1)^{t_2}}{(i+1)^{t_2} - 1} \quad (1)$$

where

C = capital cost of the system;

i = discount rate;

t_1 = system lifetime;

t_2 = HERON project runtime.

In HERON, the nuclear island is modeled with two components: a microreactor and a TES. The microreactor produces a resource called heat with a fixed dispatch. The TES component stores heat with an independent dispatch. The heat resource can be used by a BOP component to produce electricity and by an MEE component to generate purified water.

Wind generation, diesel backup, and PHS are also modeled. Wind generation dispatch is determined using an ARMA ROM. Grid electrical demand is calculated similarly with its ARMA ROM. There is also a constant water demand of 8 kg/s, which is about 10% of the island's current water demand. Both the TES and PHS storage systems have a round-trip efficiency (RTE) parameter. The RTE for the TES was set to be 99% [40], while the RTE for the PHS was set to be 43% [41]. The transfer equations used in the surrogate models for the BOP and MEE components are provided in Equations (2) and (3), respectively. These equations were created by sampling the dynamic model at several steady-state conditions and curve fitting a polynomial function to the data. The system size of the sampled model was determined using the demand data from the microgrid.

$$Q_{RX} = 2.78 \cdot W_e + 0.6335 \cdot {W_e}^2 - 0.371 \cdot {W_e}^3 + 0.0651 \cdot {W_e}^4 - 0.0037 \cdot {W_e}^5 \quad (2)$$

$$Q_{RX} = 0.2688 \cdot \dot{m}_{water} \quad (3)$$

where

Q_{RX} = reactor heat (MW_{th});
W_e = electrical power (MW_e);
$\dot{m}_{water}$ = desalinated water mass flow rate (kg/s).

Because HERON is an economic optimizer, the price of electricity and diesel affect the optimized solution. Depending on diesel prices and expected microreactor cost, there may not currently be an economic case to build a microreactor for electricity generation; however, economics is not the only driving factor. A nuclear system would further decarbonize the microgrid, as well as add more resiliency and reliability because it would not be dependent on the weather. The value of these additional factors is not easily quantifiable. For this work, the goal was to find the optimized reactor and TES configuration that would reduce the total amount of diesel used over the year to about 5% of the microgrid's current consumption.

Table 3 lists the economic values used for the reactor and TES system. All the results of this analysis are highly dependent on these costs. The cost of the microreactor is the main driver of the system's economics. Because the current cost estimates for microreactors vary greatly, the optimized results change accordingly. The price of desalinated water is set such that it breaks even with the cost of the reactor power required for the MEE system (2.16 MW_{th}).

Table 3. HERON component costs.

Component	CAPEX	OPEX	Ref
Microreactor	USD 13,000/kW_e	USD 100/MWh_e	[39]
Two-Tank Salt TES	USD 18.3/kWh_{th}	USD 3.5/MWh_{th}	[40]

3. Results

3.1. Optimization

Several HERON runs were performed to analyze the proposed system with different installation cases.

3.1.1. Diesel Pricing

Using the ARMA ROM trained on electrical demand and wind generation data from El Hierro, 1000 ARMA sets were sampled, providing 292,000 cluster samples. For each cluster, the average net demand was calculated (mean demand less mean wind generation). This distribution of net demand is plotted in Figure 11, as are two reactor sizes and the demand they are capable of fully meeting, assuming infinite no-loss storage and a constant-efficiency BOP. Clusters to the left of each reactor line can be fully satisfied by the reactor and wind without diesel. Clusters to the right require some amount of diesel to meet demand. This figure illustrates the diminishing returns of increasing reactor capacity. For clusters to the right of the reactor line, the reactor is operating at full power, and for the clusters to the

left, the reactor power must be reduced or wasted as more power is being generated than is needed. Because storage only works within a cluster, excess energy cannot be stored for another cluster with higher demand. Figure 12 shows a complementary cumulative distribution function (CCDF).

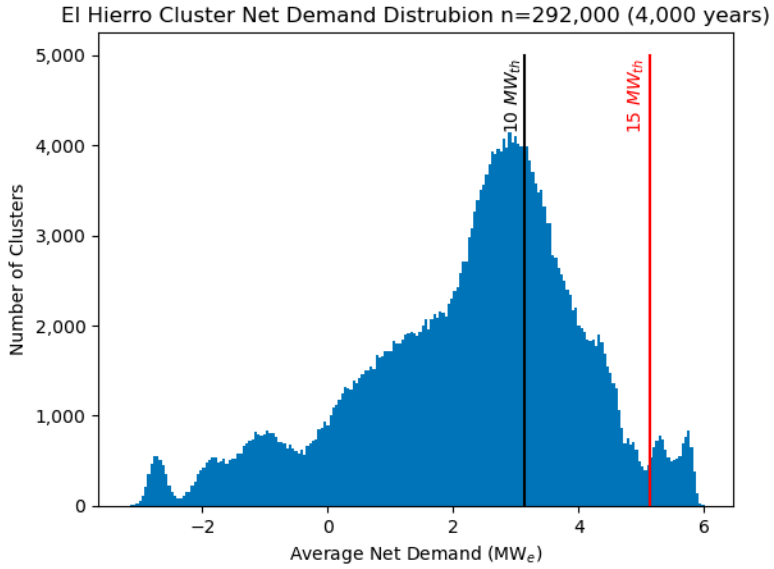

Figure 11. Net demand cluster distribution.

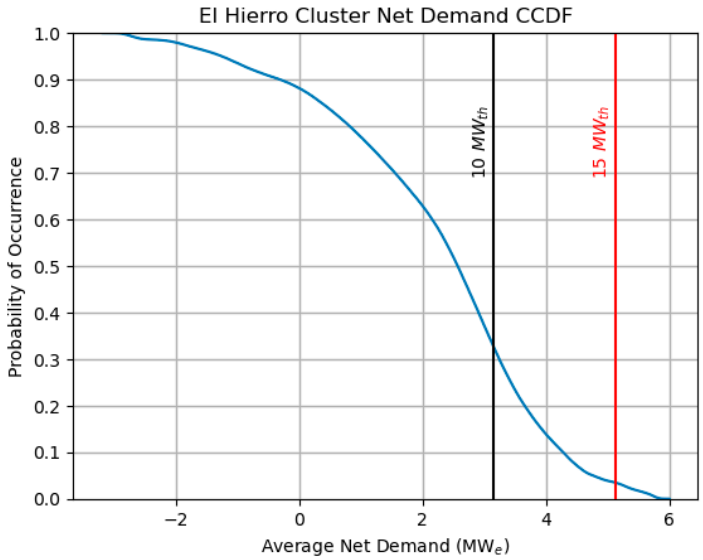

Figure 12. Net demand cluster complementary cumulative function.

For clusters where the demand is not fully met by the reactor power, most of the demand is still met. Figure 13 shows the amount of demand missed by the reactor system that would need to be made up with diesel. Assuming a constant thermal efficiency and using the distribution in Figure 12, a theoretical curve was generated. To find the actual amount, a sweep of reactor sizes was run in HERON, assuming a large TES capacity (5000 MWh_{th}). The actual missed demand is higher than the theoretical amount due to the energy loss in the TES and PHS RTEs, as well as due to the variable Rankine cycle efficiency caused by off-design operation. This shows the diminishing returns of increasing reactor capacity.

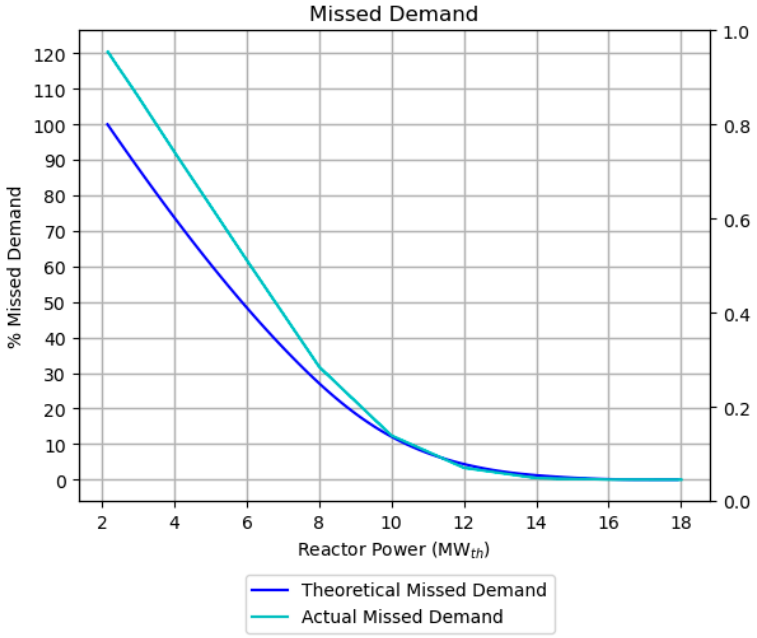

Figure 13. The amount of missed demand with different reactor sizes.

Missed demand was calculated using Equation (4).

$$MD = \frac{\overline{E}_{diesel}}{\overline{E}_{demand} - \overline{E}_{wind}} \quad (4)$$

where

MD = the percentage of demand missed by nuclear;
$\overline{E}_{diesel}$ = the average energy supplied by diesel backup;
$\overline{E}_{demand}$ = the average electrical demand of the system;
$\overline{E}_{wind}$ = the average energy supplied by wind.

To determine the price of electricity and diesel that was required to reduce the amount of diesel to about 5% of the island's current consumption, a set of optimizations was performed. The reactor and TES sizes were optimized for a range of diesel prices, and the percentage of diesel used for each case was calculated. With a diesel and electricity price of USD 993/MWh$_e$, the optimal reactor size was found to be 11.66 MW$_{th}$, and the optimal TES size was found to be 73.18 MWh$_{th}$. This combination resulted in diesel being used for 5% of the non-renewable electricity load. This diesel price is used for the remainder of the results.

3.1.2. Optimization Surface

A sweep of reactor sizes and TES capacities was run to visualize the optimization surface. This sweep allows for the smoothness of the solution space to be observed. Due to the stochastic nature of the synthetic demand profiles created by the ARMA ROMs, the optimization surface can be very rough if not enough samples are used in the inner loop. This can make it difficult for the optimizer to find the global maximum rather than a local maximum. The optimization surface (Figure 14) can also show the sensitivity of the capacities on the NPV of the system. Because all constant costs are not accounted for, such as the MEE cost, the results are shown as a Δ NPV, where the configuration with the max NPV is set equal to zero.

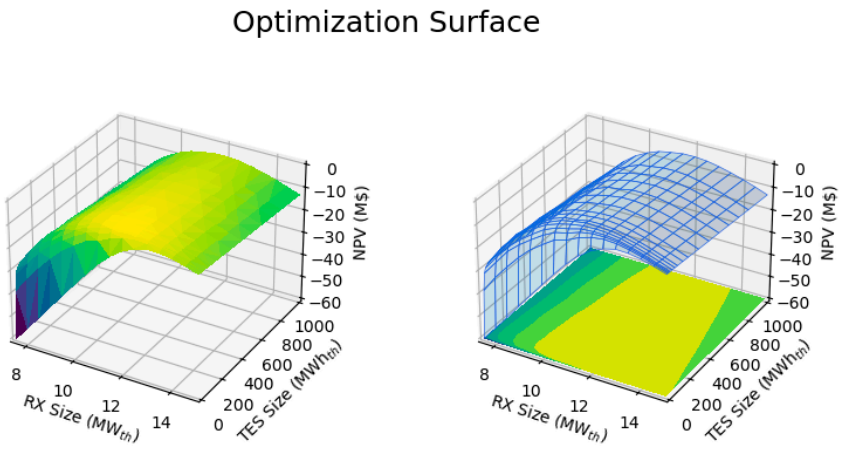

Figure 14. HERON optimization surface.

3.1.3. Full System Optimization

Due to the stochastic nature of HERON, the optimized solution for each run is different. The optimizer itself also adds uncertainty to the solution. To see this sensitivity, the same optimization was run 1000 times, leading to 1000 different optimized solutions. Figure 15 shows a scatter plot of the results and the distribution of the resulting reactor and TES sizes. The reactor power distribution is relativity tight, whereas the TES capacity shows higher variance. The NPV of each result is shown as a Δ NPV, with the point in red being the result with the max NPV. The results show a relatively large range of TES sizes, from as low as 40 MWh_{th} to 140 MWh_{th}, though most results are in the 70–120 MWh_{th} range. The reactor results are much more clustered, ranging from 11.3 to 12.5 MW_{th}. There is a clear gradient with the results for the NPV; the lower TES sizes have higher NPVs, though there is a relatively small USD 0.5M difference between the best and worst results. This shows that the optimizer tends to overestimate the size of the TES that is required. The result with the highest NPV had a reactor size of 11.61 MW_{th} and a TES size of 58.41 MWh_{th}. The standard deviation was 0.22 MW_{th} for the reactor size and 11.89 MWh_{th} for the TES system.

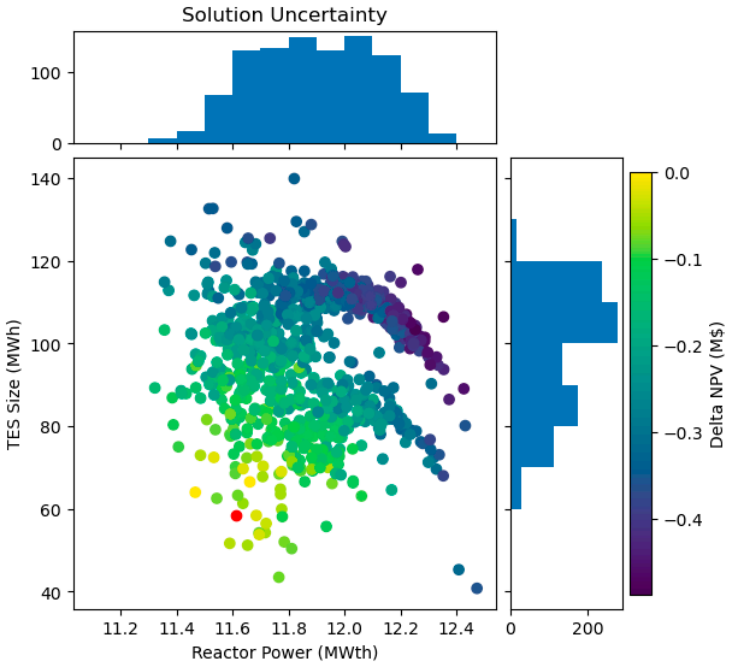

Figure 15. Optimization solution uncertainty distribution, where each point is the result of an optimization. The red point is the optimized solution with the maximum NPV.

3.1.4. Fixed Reactor Optimization

Realistically, no vendor will sell an 11.61 MW_{th} reactor. It is more likely they will be offered in a few discrete sizes. To understand the penalty for choosing a discrete reactor size, for this analysis, the TES sizes were optimized for two fixed reactor sizes: 10 MW_{th} and 15 MW_{th}.

For a 10 MW_{th} reactor, the optimized TES size is 113.1 MWh_{th}. The effect of TES size on the Δ NPV is shown in Figure 16, with the NPV of the case with no TES set equal to zero. Even a small amount of TES allowed the reactor heat to be better utilized, greatly improving the NPV. The NPV increased until the optimal point, and then it began to decrease as the marginal improvement of reactor utilization became less than the cost to install more TES. Because of the reduced reactor capacity relative to the optimal point, the diesel utilization increased from 5 to 13.4%.

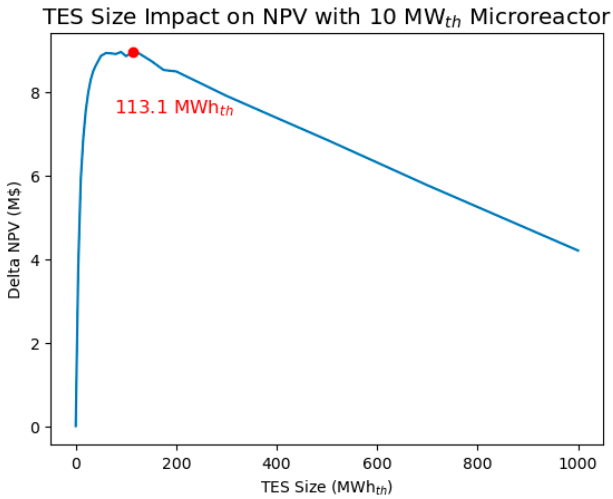

Figure 16. TES optimization surface and solution for a fixed 10 MWth reactor.

The curve for the 15 MW_{th} reactor followed a similar trend but with an optimized TES size of 14.2 MWh_{th}. This is because a 15 MW_{th} reactor was oversized for the majority of the clusters, so the TES was less useful, resulting in the relatively large size difference for the TES systems for the two cases. Because the reactor size was greater than the optimized size, diesel utilization dropped to 0.16%. As shown in Figure 17, the NPV of this case was lower than that of the 10 MW_{th} case.

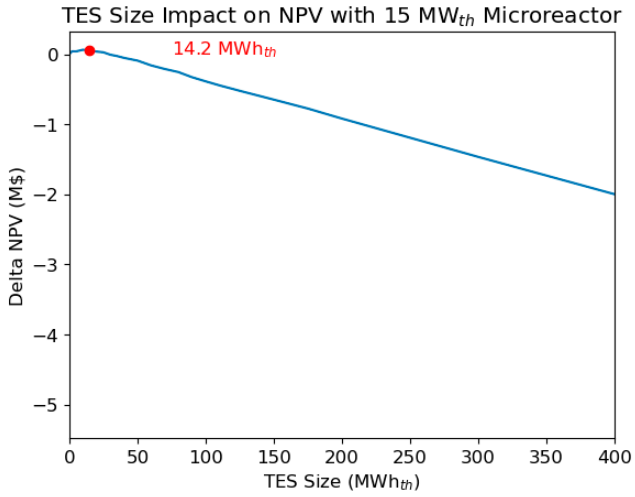

Figure 17. TES optimization surface and solution for a fixed 15 MWth reactor.

3.1.5. Dispatch

Using the optimized capacity, the dispatch for a single cluster was plotted (Figure 18a–d). Figure 18a shows the reactor heat production and usage over the course of the cluster length. The reactor produced a constant amount of heat for the entire cluster length, the MEE system used a constant amount of heat, and the turbines used a variable amount of heat depending on the electrical demand and the amount of wind generation in the system. Excess heat was stored in the TES system and dispatched later when more heat is needed.

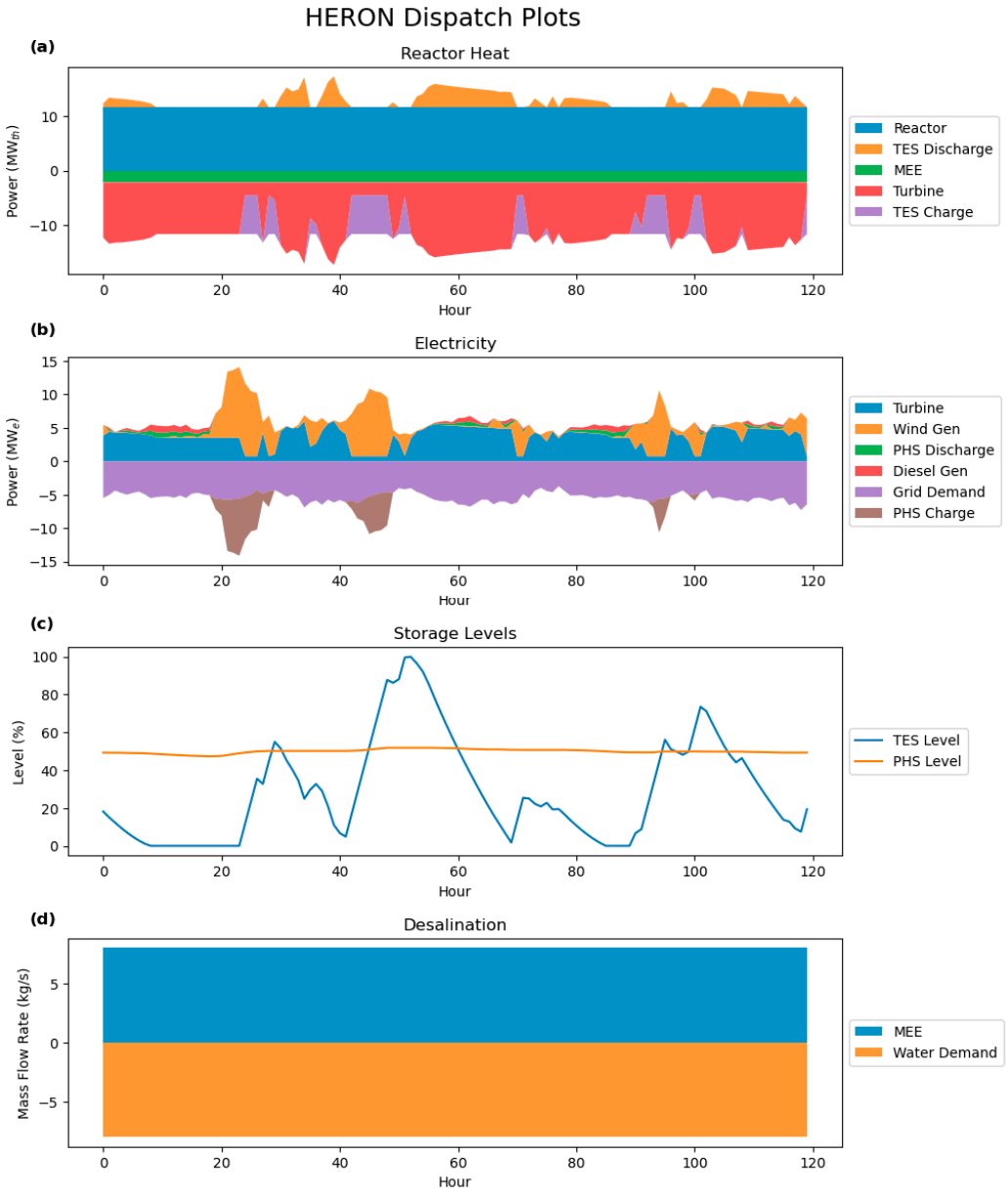

Figure 18. (**a**–**d**) HERON dispatch graphs for a single cluster.

The electricity production and usage are shown in Figure 18b. The nuclear-supplied turbine and wind turbines supplied most of the electricity production in this cluster. The wind generation was sporadic but generated a large amount of power when operating. This generation was greater than what the grid requires, so the excess was stored in the PHS system for later use. When wind generation was high, the nuclear turbine reduced power and stored the excess heat in the TES system. Both storage systems were later discharged to help meet peak demands in the cluster when there is low wind generation. Occasionally during the cluster length, wind and nuclear were not sufficient to meet demand, so diesel

backup was required. Figure 18d shows the constant water production meeting the constant water demand.

3.2. Dynamic Modeling Results

Using the capacities found with the optimization, the dynamic model can be sized and used to simulate a dispatch from the system. Using the 5-day dispatch shown in Section 3.1.5, the dynamic model was run. The initial TES level was set to the same level as that at the start of the HERON cluster. The electrical demand signal was set to be the same as the electrical demand in the HERON run minus the power from wind generation and the PHS system; the remaining electrical demand signal is the power required from the turbine and diesel backup. The Modelica model is set up to try and meet this demand as long as there is sufficient storage in the TES system. When the TES system is close to emptying, the power demand signal is reduced to prevent the tank from fully emptying.

Figure 19 shows the electrical demand signal from HERON and the dispatch from HERON and Modelica. The Modelica dispatch matched that of HERON for most of the simulation time, with a few exceptions. During the first 24 h, the Modelica model under-generated electricity. This was due to the HERON surrogate model calculating a lower heat load than the dynamic model, causing the dynamic model to empty the storage more quickly, further reducing the power output in the dynamic model. Further along in the simulation, there were several times when the Modelica power flatlined due to the physical limitations of the BOP, which were determined by the turbine sizes used in the model. This comparison indicates that HERON is likely underpredicting the amount of diesel needed. One limitation of HERON is the need for the storage level to start and end at the same level; as a result, for many of the clusters with higher power generation than demand, HERON will dump some of heat to waste when it could instead charge the TES. One important validation in this comparison is that the dynamic model can meet the high ramp rates of the system.

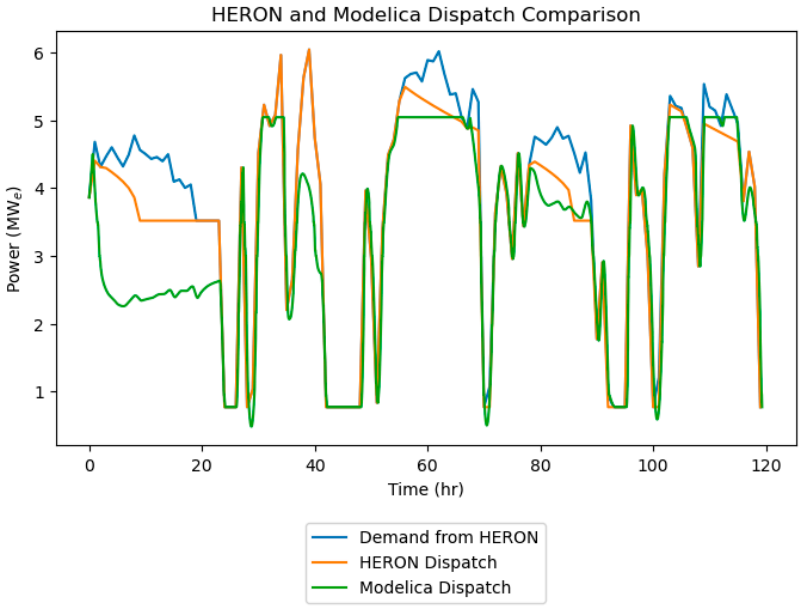

Figure 19. HERON electrical dispatch compared to dynamic model results.

Figure 20 shows the TES level of the simulation. The Modelica and HERON results match well. One notable difference occurred around the 50-h mark, when the TES level in the Modelica simulation flatlined as it approached 100% TES capacity. This was the overflow control system bypassing steam to the condenser to prevent the tank from reaching 100% capacity and overflowing. The Modelica model also ended at a slightly different

level because the Modelica simulation did not have a periodic shortage level requirement like HERON.

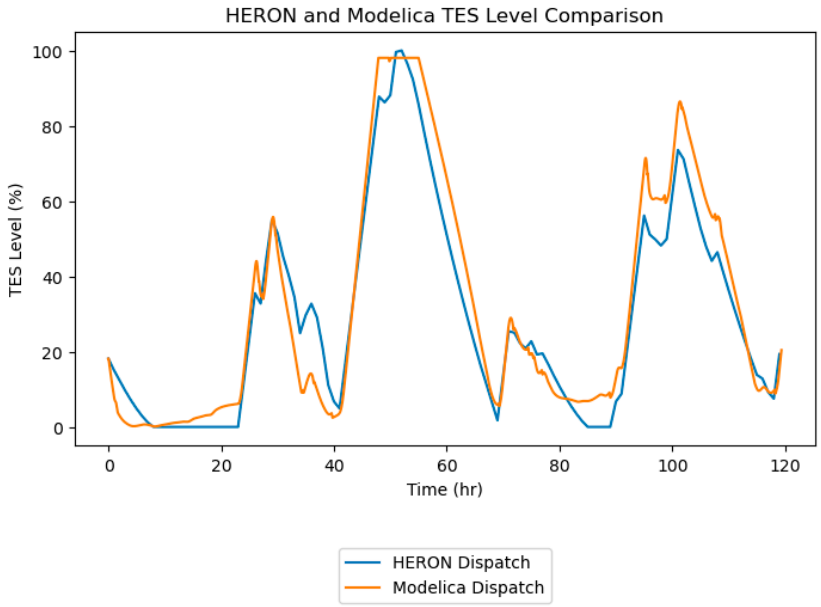

Figure 20. HERON dispatch TES level compared to dynamic model results.

The dynamic simulation was also able to meet the water demand with minor variations, as shown in Figure 21.

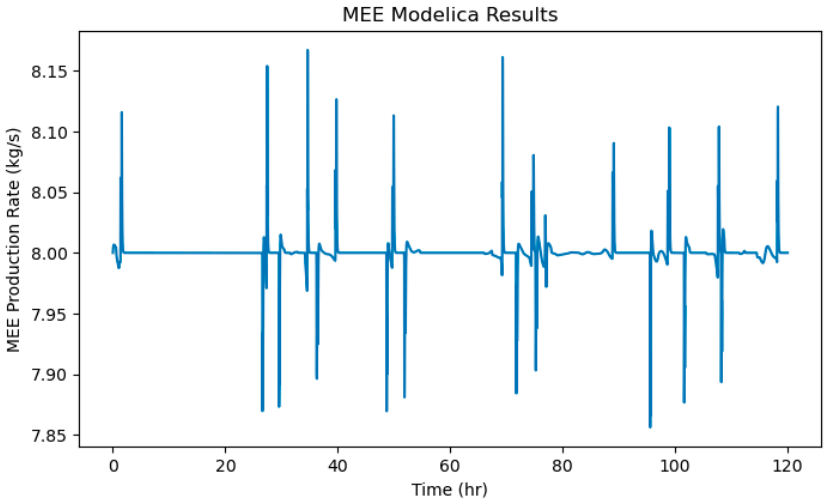

Figure 21. Dynamic model MEE results.

A benefit of running this simulation with a full reactor model is being able to analyze the reactor's response to the dynamic load of the CHP plant. Figure 22 shows the reactor power level, and Figure 23 shows the reactor control system's response. The reactor power level changed minimally throughout the simulation with little adjustment needed from the control system; this was the result of the TES system acting as a buffer between the dynamic load and the reactor.

The control system's response to achieve this low power change in the reactor can also be analyzed (see Figure 23). Both the control rods and the helium recirculator used only minimal adjustments to maintain the core power. This again shows that the primary factor stabilizing the reactor is the TES system, with its constant charge rate.

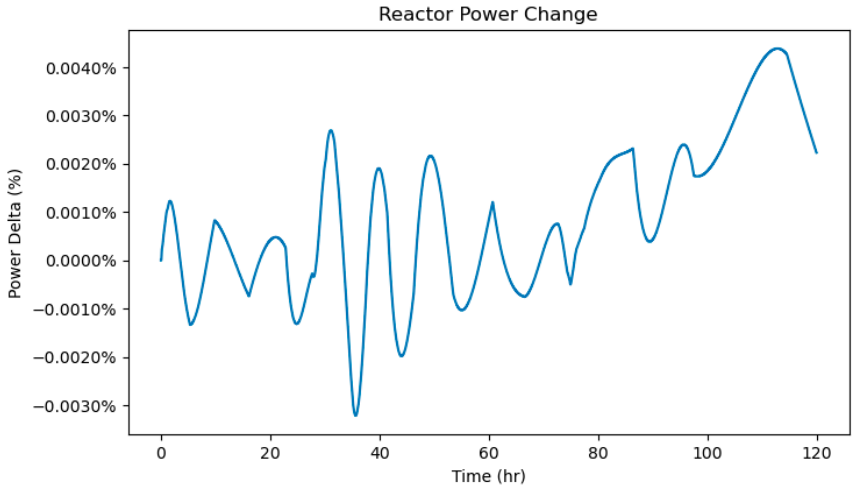

Figure 22. Dynamic model reactor power results.

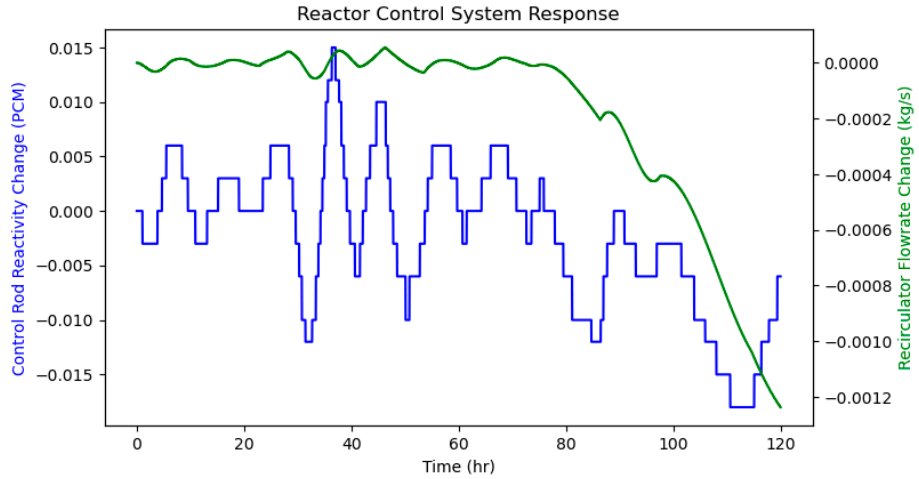

Figure 23. Dynamic model reactor control system response.

3.3. Cost of Carbon Avoided

To calculate the cost of carbon avoided for this scenario, the optimized nuclear IES was compared to the existing grid with additional desalination capacity. The additional desalination capacity was assumed to be an RO system with an efficiency of 45 kWh/m^3 and entirely powered by diesel generators.

Using the optimized reactor and TES sizes of 11.61 MW_{th} and 58.41 MWh_{th}, respectively, the annualized cost of the reactor and TES system would be USD 10.702 M/yr. This system would be able to replace 24,530 MWh_e of electricity production per year, and an additional 1000 MWh_e/yr needed for desalination. Assuming a diesel emission rate of 0.79 tCO_2/MWh, the nuclear IES would reduce the amount of CO_2 emissions of a similar diesel-powered system by 20,000 tCO_2/yr. Using the current estimated cost for this proposed nuclear system, this results in a cost of carbon avoided of USD 530/tCO_2.

4. Conclusions

This work presents a framework that can be used to optimize and evaluate nuclear IESs for remote microgrids. Using the FORCE tools, an IES powered by a nuclear microreactor was designed, optimized, and analyzed for use with the remote microgrid on the island of El Hierro, Spain.

Using an artificially high diesel price of USD 993/MWh_{th}, the mean optimal reactor and TES sizes were found to be 11.61 MW_{th} and 58.41 MWh_{th}, respectively. The standard deviation for reactor sizes was found to be only 0.22 MW_{th}, while the standard deviation

for the TES was 11.89 MWh_{th}. The TES size was also optimized for two fixed reactor sizes of 10 and 15 MW_{th}, the optimal TES sizes for each being 113.1 and 14.2 MWh_{th}, respectively. These results can help inform stakeholders' decisions on the possible implementation of a microreactor into the microgrid.

A dynamic model of the microgrid was also created using models from the HYBRID repository. These models were sized using the solution from the optimization. With this model, the output dispatch from HERON was compared to the dispatch of the dynamic model. This comparison showed reasonable matching, increasing confidence in the optimization results. The dispatch also showed that the dynamic model could meet the ramp rates while maintaining reactor power with minimal control adjustments.

There remain other challenges with implementing a microreactor power IES in a remote microgrid, such as citing, licensing, operations, and security. These issues must be addressed before such a system could be built. Despite these challenges and large costs, this system would provide clean, reliable power and provide access to more fresh water. The gird would become more resilient and the subsequent prices for electricity would be more stable and less dependent on the fluctuating price of fossil fuels.

Author Contributions: Conceptualization, L.W., J.M.D. and D.M.; methodology, L.W.; software, L.W.; validation, L.W.; formal analysis, L.W.; investigation, L.W.; resources, D.M.; data curation, L.W.; writing—original draft preparation, L.W.; writing—review and editing, L.W., D.M. and J.M.D.; visualization, L.W.; supervision, J.M.D. and D.M.; project administration, J.M.D.; funding acquisition, D.M. All authors have read and agreed to the published version of the manuscript.

Funding: This manuscript has been authored by a contractor of the U.S. Government for the U.S. Department of Energy, Office of Nuclear Energy (NE), under DOE-NE Idaho Operations Office Contract DEAC0705ID14517.

Data Availability Statement: The original contributions presented in the study are included in the article, and further inquiries can be directed to the corresponding author.

Conflicts of Interest: The authors declare no conflicts of interest.

References

1. Ton, D.T.; Smith, M.A. The U.S. Department of Energy's Microgrid Initiative. *Electr. J.* **2012**, *25*, 84–94. [CrossRef]
2. Klouda, N.; Johnson, R.; Mills, I.; Jang, H.; Worbel, A.; Minute, M. *Microreactors in Alaska Use Case Analysis: Executive Summary*; The University of Alaska Center for Economic Development: Anchorage, AK, USA, 2020; p. 6. Available online: https://static1.squarespace.com/static/59f6b60bcf81e02892fd0261/t/60189a8fc18e871112eff45b/1612225177349/Use+Case+Analysis_Executive+Summary.pdf (accessed on 30 October 2020).
3. Lovering, J.R. A Techno-Economic Evaluation of Microreactors for Off-Grid and Microgrid Applications. *Sustain. Cities Soc.* **2023**, *95*, 104620. [CrossRef]
4. Shropshire, D.; Black, G.; Araujo, K. *Global Market Analysis of Microreactors*; Office of Scientific and Technical Information (OSTI): Idaho Falls, ID, USA, 2021. [CrossRef]
5. Bragg-Sitton, S.M.; Rabiti, C.; Boardman, R.D.; O'Brien, J.E.; Morton, T.J.; Yoon, S.; Yoo, J.S.; Frick, K.L.; Sabharwall, P.; Harrison, T.J.; et al. Integrated Energy Systems: 2020 Roadmap. United States. 2020. Available online: https://www.osti.gov/biblio/1670434 (accessed on 16 October 2024).
6. Akter, A.; Zafir, E.I.; Dana, N.H.; Joysoyal, R.; Sarker, S.K.; Li, L.; Muyeen, S.M.; Das, S.K.; Kamwa, I. A review on microgrid optimization with meta-heuristic techniques: Scopes, trends and recommendation. *Energy Strategy Rev.* **2024**, *51*, 101298. [CrossRef]
7. Masrur, H.; Howlader, H.O.; Elsayed Lotfy, M.; Khan, K.R.; Guerrero, J.M.; Senjyu, T. Analysis of Techno-Economic-Environmental Suitability of an Isolated Microgrid System Located in a Remote Island of Bangladesh. *Sustainability* **2020**, *12*, 2880. [CrossRef]
8. Pecenak, Z.K.; Stadler, M.; Mathiesen, P.; Fahy, K.; Kleissl, J. Robust design of microgrids using a hybrid minimum investment optimization. *Appl. Energy* **2020**, *276*, 115400. [CrossRef]
9. Stadler, M.; Groissböck, M.; Cardoso, G.; Marnay, C. Optimizing Distributed Energy Resources and building retrofits with the strategic DER-CAModel. *Appl. Energy* **2014**, *132*, 557–567. [CrossRef]
10. Howells, M.; Rogner, H.; Strachan, N.; Heaps, C.; Huntington, H.; Kypreos, S.; Hughes, A.; Silveira, S.; DeCarolis, J.; Bazillian, M.; et al. OSeMOSYS: The Open Source Energy Modeling System: An introduction to its ethos, structure and development. *Energy Policy* **2011**, *39*, 5850–5870. [CrossRef]
11. Gabbar, H.A.; Adham, M.I.; Abdussami, M.R. Analysis of nuclear-renewable hybrid energy system for marine ships. *Energy Rep.* **2021**, *7*, 2398–2417. [CrossRef]

12. Dailey, R.; Lindley, B. Locational Variance in Nuclear Microreactor Performance Under Net Zero Microgrid Conditions. *Nucl. Sci. Eng.* **2024**, 1–23. [CrossRef]
13. Gabbar, H.A.; Abdussami, M.R.; Adham, M.I. Optimal Planning of Nuclear-Renewable Micro-Hybrid Energy System by Particle Swarm Optimization. *IEEE Access* **2020**, *8*, 181049–181073. [CrossRef]
14. Poudel, B.; McJunkin, T.R.; Kang, N.; Reilly, J.T.; Stadler, M. Small Reactors in Microgrids: Technoeconomic Analysis; United States. 1 August 2022. Available online: https://www.osti.gov/biblio/1879211 (accessed on 17 October 2024).
15. Frick, K.; Talbot, P.; McDowell, D. Framework For Optimization Of Resources And Economics Ecosystem. United States. 2022. Available online: https://www.osti.gov/doecode/biblio/74301 (accessed on 22 August 2024).
16. INL. FORCE Tool Suite. Available online: https://Ies.inl.gov/SitePages/FORCE.aspx (accessed on 4 October 2023).
17. IAEA. Advanced Reactors Information System. Available online: https://aris.iaea.org/ (accessed on 4 October 2023).
18. Santamarta, J.C.; Rubiales, I.C.; Rodríguez-Martín, J.; Cruz-Pérez, N. Water status in the Canary Islands related to energy requirements. *Energy Effic.* **2022**, *15*, 13. [CrossRef]
19. Eléctrica, R. Electricity Demand Tracking in Real Time. 2023. Available online: https://demanda.ree.es/visiona/canarias/el_hierro5m/total (accessed on 20 October 2023).
20. Google Maps. 2024. Available online: https://google.com/maps (accessed on 15 October 2024).
21. Bayoumi, S.; Ali, M.; Amin, I.; Oterkus, S.; Shawky, H.; Oterkus, E.; El Torky, R. Environmentally-driven design of a floating desalination platform (Case study: Reverse Osmosis Floating Desalination Platform of Ras Gharib, Egypt). *AIMS Energy* **2021**, *9*, 623–650. [CrossRef]
22. Saeed, R.M.; Frick, K.L.; Shigrekar, A.; Mikkelson, D.; Bragg-Sitton, S. Mapping thermal energy storage technologies with advanced nuclear reactors. *Energy Convers. Manag.* **2022**, *267*, 115872. [CrossRef]
23. Williams, L.; Kim, J.; Novotny, V.; Popli, N.; Creasman, S.; Mikkelson, D. *Thermal Extraction Modeling Within HYBRID: Nominal and Extraction Conditions in Advanced Reactor Systems*; Office of Scientific and Technical Information (OSTI): Idaho Falls, ID, USA, 2023. [CrossRef]
24. Frick, K.; Talbot, P.; Wendt, D.; Boardman, R.; Rabiti, C.; Bragg-Sitton, S.; Ruth, M.; Levie, D.; Frew, B.; Elgowainy, A.; et al. *Evaluation of Hydrogen Production Feasibility for a Light Water Reactor in the Midwest*; Office of Scientific and Technical Information (OSTI): Idaho Falls, ID, USA, 2019. [CrossRef]
25. Wendt, D.; Knighton, L.; Boardman, R. *High Temperature Steam Electrolysis Process Performance and Cost Estimates*; Office of Scientific and Technical Information (OSTI): Idaho Falls, ID, USA, 2022. [CrossRef]
26. Talbot, P.; McDowell, D.; Richards, J.; Cogliati, J.; Alfonsi, A.; Rabiti, C.; Boardman, R.; Bernhoft, S.; La Chesnaye, F.; Ela, E.; et al. *Evaluation of Hybrid FPOG Applications in Regulated and Deregulated Markets Using HERON*; Office of Scientific and Technical Information (OSTI): Idaho Falls, ID, USA, 2020. [CrossRef]
27. McDowell, D.; Talbot, P.; Wrobel, A.; Frick, K.; Bryan, H.; Boyer, C.; Boardman, R.; Taber, J.; Hansen, J. *A Technical and Economic Assessment of LWR Flexible Operation for Generation and Demand Balancing to Optimize Plant Revenue*; Office of Scientific and Technical Information (OSTI): Idaho Falls, ID, USA, 2021. [CrossRef]
28. Frick, K.; Mikkelson, D.; Alfonsi, A.; Rabiti, C. HYBRID User Manual. 2022. Available online: https://github.com/idaholab/HYBRID (accessed on 21 September 2023).
29. Epiney, A.; Rabiti, C.; Kim, J.; Frick, K.; Talbot, P.; Kinoshita, R.; Tang, Y.; Greenwood, M.; Pnciroli, R.; Alfonsi, A.; et al. Hybrid Simulation Framework. United States. 2021. Available online: https://www.osti.gov/doecode/biblio/53749 (accessed on 21 September 2023).
30. Rabiti, C.; Alfonsi, A.; Cogliati, J.; Mandelli, D.; Kinoshita, R.; Sen, S.; Wang, C.; Talbot, P.W.; Maljovec, D.P.; Abdo, M.G. *RAVEN User Manual*; Idaho National Laboratory: Idaho Falls, ID, USA, 2023. Available online: https://github.com/idaholab/raven/ (accessed on 21 September 2023).
31. Slaughter, A.; Miller, J.; Epiney, A.; Alfonsi, A.; Spencer, B.; Permann, C.; Wang, C.; Maljovec, D.; Andrs, D.; Gaston, D.; et al. Raven. United States; 2017. Available online: https://www.osti.gov/doecode/biblio/11682 (accessed on 21 September 2023).
32. Talbot, P.W.; McDowell, D.J.; Garrett, R.D.; Hanna, B.N.; Gairola, A.; Zhou, J.; Griffith, A.; Soto, G.J. *HERON User Manual*; Idaho National Laboratory: Idaho Falls, ID, USA, 2023. Available online: https://github.com/idaholab/HERON/ (accessed on 21 September 2023).
33. Talbot, P.; Rabiti, C.; Gairola, A.; Frick, K.; Prateek, P.; Zhou, J. HERON. United States; 2020. Available online: https://www.osti.gov/doecode/biblio/45038 (accessed on 21 September 2023).
34. Talbot, P.; Gairola, A.; Prateek, P.; Alfonsi, A.; Rabiti, C.; Boardman, R. *HERON as a Tool for LWR Market Interaction in a Deregulated Market*; INL/EXT-19-56933; INL: Idaho Falls, ID, USA, 2019.
35. Williams, L.; Mikkelson, D.; Doster, J.M. Prismatic High Temperature Gas-Cooled Reactor Model in Support of Integrated Energy Systems. In Proceedings of the 2024 International Congress on Advances in Nuclear Power Plants, Las Vegas, NV, USA, 16–19 June 2024; pp. 624–633. [CrossRef]
36. Williams, L.; Solis, E.; Terry, S.; Doster, J.M.; Mikkelson, D. Modeling Cogeneration Systems to Produce Electrical Power and Drinking Water. *Altern. Energy Distrib. Gener. J.* **2023**, *5*, 7–35.
37. Kim, J.S.; Frick, K. *Status Report on the Component Models Developed in the Modelica Framework: Reverse Osmosis Desalination Plant & Thermal Energy Storage*; Office of Scientific and Technical Information (OSTI): Idaho Falls, ID, USA, 2018. [CrossRef]

38. Frick, K.L.; Doster, J.M.; Bragg-Sitton, S.M. Auxiliary Feedwater Reheating to Mitigate Primary and Secondary Side Thermal Stressors. In Proceedings of the 11th Nuclear Plant Instrumentation, Control and Human-Machine Interface Technologies (NPIC&HMIT) 2019, Orlando, FL, USA, 23 January 2019. Available online: https://www.osti.gov/biblio/1498075 (accessed on 30 October 2024).
39. Abou-Jaoude, A.; Lin, L.; Bolisetti, C.; Worsham, E.K.; Larsen, L.M.; Epiney, A.S. Literature Review of Advanced Reactor Cost Estimates; United States. 2023. Available online: https://www.osti.gov/biblio/1986466 (accessed on 10 June 2024).
40. Gautam, K.R.; Andresen, G.B.; Victoria, M. Review and Techno-Economic Analysis of Emerging Thermo-Mechanical Energy Storage Technologies. *Energies* **2022**, *15*, 6328. [CrossRef]
41. Briongos, F.; Platero Gaona, C.A.; Sánchez-Fernández, J.A. Increasing Demand Covered by Renewable Energy in El Hierro Island. *Sustainability* **2023**, *15*, 16185. [CrossRef]